Consequences of Oxygen-Vacancy Correlations at the SrTiO_{3} Interface

Chungwei Lin and Alexander A. Demkov

Phys. Rev. Lett. **113**, 157602 — Published 8 October 2014

DOI: 10.1103/PhysRevLett.113.157602

Consequences of Oxygen Vacancy Correlations at the $SrTiO_3$ Interface

Chungwei Lin and Alexander A. Demkov*
Department of Physics, University of Texas at Austin, Austin, Texas 78712, USA
(Dated: September 17, 2014)

The Kondo effect and ferromagnetism are the two many-body phenomena that emerge at the $SrTiO_3$ interfaces with polar materials, but do not occur in bulk $SrTiO_3$. By regarding the oxygen vacancy (OV) in $SrTiO_3$ as a magnetic impurity, we show that these two interface specific phenomena can be attributed to the vacancies residing in the top TiO_2 plane of $SrTiO_3$. We identify three crucial ingredients the local orbital mixing caused by an OV, reduced symmetry at the interface, and strong in-plane stray electric field of the polar material. All three factors combine to result in the coupling between the impurity and conduction band at the interface, and can lead to both emergent phenomena. An OV-based Anderson impurity model is derived and solved using the numerical renormalization group method. The Kondo and Curie temperatures are estimated. Several experiments based on this interpretation are discussed.

PACS numbers: 79.60.Dp, 71.55.-i, 71.27.+a

Perovskite $SrTiO_3$ (STO) is a non-magnetic band insulator with a band gap of 3.2 eV [1, 2]. Its versatile response to different dopants makes STO an ideal host for building functional materials and has drawn significant attention. For example, an insulating ferromagnetic (FM) order at room temperature is observed in STO when replacing some Ti atoms by Co [3, 4]. The band gap of STO can be engineered by Al doping [5]. When a small number of conduction electrons are introduced, even more fascinating phenomena such as superconductivity [6–8], long-lived magnetic moments [9], metallic ferromagnetism or super-paramagnetism (SPM, several separate macroscopic FM domains) [10–15], Kondo resistance minimum [16–18], and two-dimensional electron gas [19–22] emerge. Among these emergent phenomena, the ferromagnetism and Kondo effect are special in that they, unlike the superconductivity, only occur at the STO/$LaAlO_3$ (LAO) (for FM) [10–13, 23], and STO/ionic liquid interfaces (for Kondo effect) [17, 18, 24], but do not occur in the n-doped bulk STO [25–30]. In this letter, we investigate the role of oxygen vacancies (OV) in these two phenomena. We find the OV, residing in the top TiO_2 plane, plays an important role in distinguishing the interface behavior from the bulk. By regarding OVs in STO as magnetic impurities [31], we identify three crucial ingredients necessary for FM and Kondo effect to occur – (i) local orbital mixing at the adjacent Ti sites caused by an OV, (ii) symmetry reduction near the interface, and (iii) strong in-plane stray electric field induced by the polar interface. A combination of these three factors results in an impurity-conduction band coupling near the interface and can lead to the emergent FM phase and Kondo effect.

We begin by summarizing the key features of an OV in STO from the density functional theory (DFT) [32–38]. The conduction bands of bulk STO are mainly derived from Ti $3d$ orbitals, with triple-degenerate t_{2g} bands about 2.5 eV below the double-degenerate e_g bands in energy. When an OV between two Ti sites at $\mathbf{R}$ and $\mathbf{R}+\hat{x}$ is introduced, the local symmetry is reduced from cubic to C_{4v}, and induces a strong coupling between $|\mathbf{R};3d_{3x^2-r^2}\rangle$ and $|\mathbf{R};4p_x\rangle$ unperturbed orbitals. The resulting local hybrid state, denoted as $|\mathbf{R};3d_{3\bar{x}^2-\bar{r}^2}\rangle$, can be approximated by

$$|\mathbf{R}(+\hat{x});3d_{3\bar{x}^2-\bar{r}^2}\rangle = \sqrt{1-\alpha^2}|\mathbf{R};3d_{3x^2-r^2}\rangle + (-)\alpha|\mathbf{R};4p_x\rangle. \quad (1)$$

By comparing the relative $3d$ and $4p$ contributions to the OV-induced peak in the density of states (DOS) [38],

* E-mail: demkov@physics.utexas.edu

we estimate $\alpha \approx 1/\sqrt{5}$. Compared to the $|\mathbf{R}; 3d_{3x^2-r^2}\rangle$ orbital, the $|\mathbf{R}; 3d_{3\bar{x}^2-\bar{r}^2}\rangle$ hybrid is about 1.0 eV lower in energy and has an asymmetric shape due to the appreciable Ti $4p_x$ component. This spatially extended $4p_x$ character allows for the hybridization between the two $|3d_{3\bar{x}^2-\bar{r}^2}\rangle$ hybrids across an OV. Their bonding combination, $|\{\mathbf{R}, x\}; b\rangle = \left(|\mathbf{R}; 3d_{3\bar{x}^2-\bar{r}^2}\rangle + |\mathbf{R}+\hat{x}; 3d_{3\bar{x}^2-\bar{r}^2}\rangle\right)/\sqrt{2}$, gives the lowest OV-induced single-particle level [see Fig. 1(a)]. We shall use $\{\mathbf{R}, a\}$ ($a = x$ or y) to label the OV between $\mathbf{R}$ and $\mathbf{R}+\hat{a}$. For physics at low temperature, what an OV does is to introduce the bonding state, which will be referred to as the OV-induced impurity state, or simply the impurity state. Because the OV-induced impurity level is below the conduction band [22, 39] and is spatially localized, it is always half-filled due to the strong on-site repulsion [31]. The nominal charge configuration can be approximated by Ti^{4+}-OV^{1-}-Ti^{4+}, or more precisely by $Ti^{3.5+}$-OV^{0}-$Ti^{3.5+}$ [31, 35].

We now discuss the coupling between the impurity level and the t_{2g} ($3d_{xy}$ in particular) conduction band (also referred to as bath). Due to its spatial extension, the impurity orbital only significantly overlaps with two Ti $3d_{xy}$ orbitals adjacent to the vacancy [see Fig. 2(a)]. The coupling can be described by the tight-binding approximation as

$$\begin{aligned} -g &= \langle \mathbf{R}; 3d_{xy}|\Delta U|\{\mathbf{R}, x\}; b\rangle \\ &= \frac{\sqrt{1-\alpha^2}}{\sqrt{2}}\langle \mathbf{R}; 3d_{xy}|\Delta U|\mathbf{R}; 3x^2-r^2\rangle + \frac{\alpha}{\sqrt{2}}\langle \mathbf{R}; 3d_{xy}|\Delta U|\mathbf{R}; 4p_x\rangle, \end{aligned} \tag{2}$$

with ΔU the difference between the atomic and lattice potentials [40]. As $g = 0$ under the C_{4v} symmetry (x being the rotation axis), the OV in the bulk is decoupled from the conduction bands, except providing a scattering potential [41]. Therefore, despite its spin degree of freedom, an OV in the bulk does not result in any magnetism-related many-body effects.

In contrast, there are two mechanisms leading to a non-zero g for vacancies located in the top TiO_2 x-y plane (z defines the surface normal). First, the non-inversion symmetric environment ($\pm z$ are inequivalent) at the interface induces a non-zero coupling between OV and $3d_{xz}/3d_{yz}$ orbitals. To have a non-zero OV-$3d_{xy}$ coupling, local C_2 symmetry has to be lifted. This can happen easily in the region of high OV concentration, where the equilibrium position of the Ti atom deviates from the Ti-OV-Ti axis due to another OV nearby. Second, when STO is in contact with a polar material such as LAO or ionic liquid, the in-plane stray field, caused by the inhomogeneous interface charges, also leads to a non-zero g. For the interface stray field [see Fig. 1(b)], locally approximated by the potential $V_{int} = -Ey$, the coupling is given by

$$-g = \frac{\alpha}{\sqrt{2}}\langle 3d_{xy}|V_{int}|3d_{3\bar{x}^2-\bar{r}^2}\rangle = \frac{-E\alpha}{\sqrt{2}}\langle 3d_{xy}|y|4p_x\rangle, \tag{3}$$

where we take $\mathbf{R} = 0$ and neglect the position label for simplicity [42]. Note that the x and z components of the stray field do not induce the coupling because $\langle 3d_{xy}|x|4p_x\rangle = \langle 3d_{xy}|z|4p_x\rangle = 0$. Using the atomic wave functions with an effective Bohr radius of 2.0 Å [43] and taking the strength of a stray field to be $E = 0.5$ V/Å [44], we estimate $g \sim 0.2$ eV. Three features of this mechanism are emphasized. First, it is the Ti $4p$ component of the impurity level that couples to the conduction band via the external field. Second, it is the in-plane component of the stray field that contributes to the coupling, so the inhomogeneity of the surface charge distribution is essential [45]. Third, the stray field decays, and its effect is only noticeable within one or two unit cells away from the interface [46]. In reality we believe the both mechanisms contribute to the non-zero impurity-bath coupling, which is the very factor distinguishing the interface behavior from the bulk.

An OV-based Anderson impurity model [47] at the STO interface is now derived. It has been established that near the interface, the $3d_{xy}$-based band is the lowest in energy because occupying this band screens the external field most efficiently [22, 37, 48–50]. To investigate the OV effect, we have proposed an AIM where the bath orbitals are composed of Ti $3d$ and O $2p$ orbitals [Fig. 2(a)]. For physics at low temperature, the bath can be further simplified

by including only the $3d_{xy}$ orbitals [Fig. 2(b)]. The OV-based AIM, $H_{AIM} = H_{bath} + H_{OV}$, contains two parts. The conduction band is $H_{bath} = \sum_{\mathbf{k}} \sum_{\sigma} \varepsilon(\mathbf{k}) c^{\dagger}_{\mathbf{k},\sigma} c_{\mathbf{k},\sigma}$, with $c_{\mathbf{k},\sigma}$ the annihilation operator of Ti $3d_{xy}$ orbital. Using the tight-binding dispersion $\varepsilon_{\mathbf{k}} = -2t(\cos k_x + \cos k_y)$ with $t = 0.25$ eV (the band width is 2.0 eV), one estimates the DOS $\rho_0 \sim 0.32$/eV (per spin per site) near the conduction band bottom. H_{OV} is given by

$$H_{OV}(\{\mathbf{R}, a\}) = \epsilon_b (n^{imp}_{\{\mathbf{R},a\},\uparrow} + n^{imp}_{\{\mathbf{R},a\},\downarrow}) + U n^{imp}_{\{\mathbf{R},a\},\uparrow} n^{imp}_{\{\mathbf{R},a\},\downarrow} - \sqrt{2} g \sum_{\sigma} \left[d^{\dagger}_{\{\mathbf{R},a\},\sigma} c_{\{\mathbf{R},a\},\sigma} + h.c. \right], \tag{4}$$

where $d_{\{\mathbf{R},a\}}$ is the annihilation operator of the impurity orbital, and $c_{\{\mathbf{R},a\},\sigma} = \frac{1}{\sqrt{2}} (c_{\mathbf{R},\sigma} + c_{\mathbf{R}+\hat{a},\sigma})$ is that of the bonding combination of two adjacent Ti $3d_{xy}$ orbitals. Note that the impurity level has a filling close to one, so its on-site repulsion must be included [51]. In Eq. (4) we assume that couplings between the OV and two adjacent Ti $3d_{xy}$ orbitals are identical. This corresponds to the opposite in-plane electric fields at these two Ti sites due to the character of $3d_{xy}$ orbital [52]. If the couplings have opposite sign, the impurity couples to the top of the conduction band and plays little role in the low-filling case. Based on our bulk DFT calculation [31, 36, 38], we use $U = 1.6$ eV, $\epsilon_b = -0.8$ eV, and $g = 0.2$ eV in our calculation.

To allow for a many-body simulation, we further approximate the conduction band by a constant DOS of the bandwidth $2D$, with the half bandwidth $D \sim 0.2$ eV being the energy difference between Fermi energy and conduction band bottom (inset of Fig. 3). This approximation discards states of energies higher than $2D \sim 0.4$ eV (about 4600 K), which have little effects on the physics below 100 K. Applying the numerical renormalization group (NRG) to the proposed AIM [53–57], we compute the magnetic susceptibility χ_{imp}, specific heat C_{imp}, and entropy S_{imp} due to a single OV as a function of temperature. The results are shown in Fig. 3. At high temperature, the impurity behaves like an isolated spin whose $\chi_{imp} \sim 1/T$ and $S_{imp} \sim k_B \log 2$. At low temperature the ground state is a spin-singlet which quenches the impurity entropy such that $S_{imp} \to 0$. The Kondo temperature (T_K) is determined by $T_K = w/\left[4\chi_{imp}(T=0)/(g\mu_B)^2\right]$, with $w \approx 0.413$ (Wilson number), and is estimated to be 0.15 K. The Wilson ratio $W = T\chi_{imp}/C_{imp}$ is computed to be two, placing this AIM in the Kondo regime [58]. We note that the Kondo effect neglects the impurity-impurity interaction, so its physical consequences are valid for low impurity concentration.

Now we consider the electron-mediated magnetic coupling between two impurities. In the Kondo regime, the AIM can be mapped to a Kondo model, where the impurity is simplified to a local spin $\mathbf{S}$ ($|\mathbf{S}| = 1/2$) which couples to the conduction band [59]. As the impurity lies between two Ti sites, the local spin couples to its two neighboring Ti $3d_{xy}$ orbitals and is approximated by

$$H_{spin}(\{\mathbf{R}, a\}) = \frac{J}{2} \sum_{\alpha\beta} \mathbf{S}_{\{\mathbf{R},a\}} \cdot \boldsymbol{\sigma}_{\alpha\beta} c^{\dagger}_{\{\mathbf{R},a\},\alpha} c_{\{\mathbf{R},a\},\beta} \tag{5}$$

with $J = -\frac{4(\sqrt{2}g)^2}{|\epsilon_b|} = 0.4$ eV [60]. Note that J being negative implies an anti-ferromagnetic (AF) coupling between the local spin and the conduction electrons. The magnetic coupling between two impurity spins, $\mathbf{S}_{\{\mathbf{0},x\}}$ and $\mathbf{S}_{\{\mathbf{R},a\}}$, can be computed by treating $H_{spin}(\{\mathbf{0}, x\}) + H_{spin}(\{\mathbf{R}, a\})$ as a perturbation to the band Hamiltonian [61–64]. The result, known as the Ruderman-Kittel-Kasuya-Yosida (RKKY) interaction, is typically expressed by an effective Hamiltonian, $H_{RKKY} = J_{RKKY,xa}(\mathbf{R})\, \mathbf{S}_{\{\mathbf{0},x\}} \cdot \mathbf{S}_{\{\mathbf{R},a\}}$ [65]. The negative, positive values of $J_{RKKY,xa}(\mathbf{R})$ respectively indicate the FM, AF couplings between two impurity spins. Using the Heisenberg model $J_{RKKY} \sum_{i,j} \mathbf{S}_i \cdot \mathbf{S}_j$ (assuming the spins form a lattice of some kind) to estimate the Curie temperature T_c, one gets $T_c = \frac{-qJ_{RKKY}}{4}$ with q the number of nearest neighbor. Therefore $-J_{RKKY,xa}(\mathbf{R})$ is roughly the Curie temperature. Using the same tight-binding band, the RKKY coupling [65] along three different directions are given in Fig. 4. We first note that the coupling decays and oscillates as the inter-impurity distance increases, and the oscillating period is roughly $L \sim \pi/k_F$ (k_F the Fermi wave vector). Moreover, the magnetic coupling at short distance (within three lattice constants) is FM [66], and the corresponding T_c is much higher than T_K. Our results thus suggest the local FM domain can form in the region of

high OV concentration at relatively high temperature (30-50 K), but a global FM order is difficult to achieve because the long-range magnetic coupling is weak and can be anti-ferromagnetic. Generally, the lower filling [Fig. 4 (a)] favors the FM domain formation because of the wider range of FM coupling.

Based on the provided picture we discuss several experiments related to the FM and Kondo effect near the STO interface. Before being specific, we notice that in almost all literature [10, 17, 18, 67, 68], the magnetic impurities near the interface are claimed to be Ti^{3+}. Our analysis suggests that an OV can provide an alternative explanation. We begin by discussing the STO/ionic liquid interface and the Kondo effect [17, 18]. With our theory, the OVs serve simultaneously as the electron donors and the magnetic impurities causing the Kondo effect. The estimated T_K is about ten times smaller than those obtained in Ref. [18], but the T_K depends very sensitively on the DOS and coupling strength, and a small increase in ρ_0 or J (by taking the distortion into account for example) can considerably raise T_K. Second we discuss ferromagnetism at the STO/LAO interface. Our RKKY calculation suggests that FM domains are easier to form in the interface regions of higher OV concentrations, and the T_c can be as high as 50 K, quite consistent with observations in Refs. [11, 12]. We point out that our model does not quantitatively distinguish the ionic liquid from LAO. Generally, the Kondo effect requires fewer magnetic impurities but a stronger impurity-bath coupling, whereas the RKKY-based FM requires more magnetic impurities but only a modest coupling strength. Compared to LAO, the ionic liquid interface provides a stronger stray field (due to its more irregular interface), which makes the Kondo effect observable. However, depending on the vacancy distribution, both Kondo and FM domains in principle can occur at the STO/polar material interfaces. Finally, we comment on the x-ray absorption spectroscopy of STO/LAO interface [67, 68]. The experiments show OVs are crucial to the existence of magnetic impurities, consistent with that OVs are magnetic impurities. In Ref. [67] a peak at 1.0 eV below the conduction band is observed and interpreted as Ti $3d_{xy}$ orbital. We would regard this peak as an OV-induced impurity level, composing mainly of Ti e_g and $4p$ orbitals. In Ref. [68], opposite magnetic moments of itinerant and localized spin are observed, in agreement with the AF coupling between the conduction electron and the OV spin state.

To conclude, we investigate the consequences of OV correlation in STO. In the bulk, the symmetry prevents the OV impurity state from coupling to the conduction band, and OVs are simply electron donors. Near the interface, the combination of the low symmetry environment and the strong stray field generated by the polar material results in a non-zero impurity-bath coupling, which can lead to the Kondo effect and FM/SPM phase. We emphasize two effects of the $4p$ component of the impurity level. First, it is the spatially extended character of the Ti $4p$ orbital that makes the bonding combination of two Ti hybrid states an in-gap state. Second, near the interface it is again the $4p$ component which allows for the impurity-bath coupling via the stray field. The $4p$ character of the impurity level, stemming from the local C_{4v} symmetry, in many respects is the very key that accounts for the emergent phenomena related to magnetism near the polar interface.

Acknowledgement

C.L. thanks Hoa Nghiem for helps on NRG algorithm, Yuan Ren for discussion on the stray field, and Shirin Mozaffari for discussion on the Kondo effect. We thank Kaji Lai, Andrew Millis and Allan MacDonald for a few stimulating discussions, Richard Hatch and Agham Posadas for many helpful conversations. Support for this work was provided through Scientific Discovery through Advanced Computing (SciDAC) program funded by U.S. Department of Energy, Office of Science, Advanced Scientific Computing Research and Basic Energy Sciences under award number DESC0008877.

[1] K. van Benthema, C. Elsasser, and R. H. French, J. Appl. Phys. **90**, 6156 (2001).

[2] S. Zollner, A. Demkov, R. Liu, P. Fejes, R. Gregory, P. Alluri, J. Curless, Z. Yu, J. Ramdani, R. Droopad, et al., J. Vac. Sci. Technol. B **18**, 2242 (2000).

[3] D. H. Kim, L. Bi, P. Jiang, G. F. Dionne, and C. A. Ross, Phys. Rev. B **84**, 014416 (2011), URL http://link.aps.org/doi/10.1103/PhysRevB.84.014416.

[4] A. B. Posadas, C. Mitra, C. Lin, A. Dhamdhere, D. J. Smith, M. Tsoi, and A. A. Demkov, Phys. Rev. B **87**, 144422 (2013), URL http://link.aps.org/doi/10.1103/PhysRevB.87.144422.

[5] A. B. Posadas, C. Lin, A. A. Demkov, and S. Zollner, Appl. Phys. Lett. **103**, 142906 (2013), URL http://dx.doi.org/10.1063/1.4824023.

[6] J. F. Schooley, W. R. Hosler, and M. L. Cohen, Phys. Rev. Lett. **12**, 474 (1964), URL http://link.aps.org/doi/10.1103/PhysRevLett.12.474.

[7] C. S. Koonce, M. L. Cohen, J. F. Schooley, W. R. Hosler, and E. R. Pfeiffer, Phys. Rev. **163**, 380 (1967), URL http://link.aps.org/doi/10.1103/PhysRev.163.380.

[8] N. Reyren, S. Thiel, A. D. Caviglia, L. F. Kourkoutis, G. Hammerl, C. Richter, C. W. Schneider, T. Kopp, A.-S. Ruetschi, D. Jaccard, et al., Science **317**, 1196 (2007).

[9] W. D. Rice, P. Ambwani, M. Bombeck, J. D. Thompson, C. Leighton, and S. A. Crooker, Nat. Mater. **13**, 481 (2014).

[10] A. Brinkman, M. Huijben, M. van Zalk, J. Huijben, U. Zeitler, J. C. Maan, W. G. van der Wiel, G. Rijnders, D. H. A. Blank, and H. Hilgenkamp, Nat. Mater. **6**, 493 (2007).

[11] L. Li, C. Richter, J. Mannhart, and R. C. Ashoori, Nat. Phys. **7**, 762 (2011).

[12] J. A. Bert, B. Kalisky, C. Bell, M. Kim, Y. Hikita, H. Y. Hwang, and K. A. Moler, Nat. Phys. **7**, 767 (2011).

[13] B. Kalisky, J. A. Bert, B. B. Klopfer, C. Bell, H. K. Sato, M. Hosoda, Y. Hikita, H. Y. Hwang, and K. A. Moler, Nat. Commun. **3**, 922 (2012), URL http://dx.doi.org/10.1038/ncomms1931.

[14] N. Pavlenko, T. Kopp, E. Y. Tsymbal, J. Mannhart, and G. A. Sawatzky, Phys. Rev. B **86**, 064431 (2012), URL http://link.aps.org/doi/10.1103/PhysRevB.86.064431.

[15] N. Pavlenko, T. Kopp, and J. Mannhart, Phys. Rev. B **88**, 201104 (2013), URL http://link.aps.org/doi/10.1103/PhysRevB.88.201104.

[16] J. Kondo, Prog. Theor. Phys. **32**, 37 (1964).

[17] M. Lee, J. R. Williams, S. Zhang, C. D. Frisbie, and D. Goldhaber-Gordon, Phys. Rev. Lett. **107**, 256601 (2011), URL http://link.aps.org/doi/10.1103/PhysRevLett.107.256601.

[18] M. Li, T. Graf, T. D. Schladt, X. Jiang, and S. S. P. Parkin, Phys. Rev. Lett. **109**, 196803 (2012), URL http://link.aps.org/doi/10.1103/PhysRevLett.109.196803.

[19] A. Ohtomo and H. Y. Hwang, Nature **427**, 423 (2004).

[20] S. Thiel, G. Hammerl, A. Schmehl, C. W. Schneider, and J. Mannhart, Science **313**, 1942 (2006).

[21] A. F. Santander-Syro, O. Copie, T. Kondo, F. Fortuna, S. Pailhes, W. R., X. G. Qiu, F. Bertran, A. Nicolaou, A. Taleb-Ibrahimi, et al., Nature **469**, 189 (2011).

[22] W. Meevasana, P. D. C. King, R. H. He, S.-K. Mo, M. Hashimoto, A. Tamai, P. Songsiriritthigul, F. Baumberger, and Z.-X. Shen, Nature Mater. **10**, 114 (2011).

[23] A. J. Millis, Nat. Phys. **7**, 749 (2011).

[24] Note that, although in Ref [10] the resistance minimum is observed, the Kondo effect is not well established at the $SrTiO_3/LaAlO_3$ interface, as the magnitude of the upturn appears to be too large.

[25] Y. Tokura, Y. Taguchi, Y. Okada, Y. Fujishima, T. Arima, K. Kumagai, and Y. Iye, Phys. Rev. Lett. **70**, 2126 (1993), URL http://link.aps.org/doi/10.1103/PhysRevLett.70.2126.

[26] T. Higuchi, T. Tsukamoto, K. Kobayashi, Y. Ishiwata, M. Fujisawa, T. Yokoya, S. Yamaguchi, and S. Shin, Phys. Rev. B **61**, 12860 (2000), URL http://link.aps.org/doi/10.1103/PhysRevB.61.12860.

[27] J. Inaba and T. Katsufuji, Phys. Rev. B **72**, 052408 (2005), URL http://link.aps.org/doi/10.1103/PhysRevB.72.052408.

[28] E. Ertekin, V. Srinivasan, J. Ravichandran, P. B. Rossen, W. Siemons, A. Majumdar, R. Ramesh, and J. C. Grossman,

Phys. Rev. B **85**, 195460 (2012), URL http://link.aps.org/doi/10.1103/PhysRevB.85.195460.

[29] A. Verma, A. P. Kajdos, T. A. Cain, S. Stemmer, and D. Jena, Phys. Rev. Lett. **112**, 216601 (2014), URL http://link.aps.org/doi/10.1103/PhysRevLett.112.216601.

[30] M. Choi, A. B. Posadas, C. A. Rodriguez, A. O'Hara, H. Seinige, A. J. Kellock, M. M. Frank, M. Tsoi, S. Zollner, V. Narayanan, et al., J. Appl. Phys. **116**, 043705 (2014), URL http://scitation.aip.org/content/aip/journal/jap/116/4/10.1063/1.4891225.

[31] C. Lin and A. A. Demkov, Phys. Rev. Lett. **111**, 217601 (2013), URL http://link.aps.org/doi/10.1103/PhysRevLett.111.217601.

[32] D. Ricci, G. Bano, G. Pacchioni, and F. Illas, Phys. Rev. B **68**, 224105 (2003).

[33] W. Luo, W. Duan, S. G. Louie, and M. L. Cohen, Phys. Rev. B **70**, 214109 (2004).

[34] J. Carrasco, F. Illas, N. Lopez, E. A. Kotomin, Y. F. Zhukovskii, R. A. Evarestov, Y. A. Mastrikov, S. Piskunov, and J. Maier, Phys. Rev. B **73**, 064106 (2006).

[35] Z. Hou and K. Terakura, J. Phys. Soc. Japan **79**, 114704 (2010).

[36] C. Mitra, C. Lin, J. Robertson, and A. A. Demkov, Phys. Rev. B **86**, 155105 (2012), URL http://link.aps.org/doi/10.1103/PhysRevB.86.155105.

[37] J. Shen, H. Lee, R. Valentí, and H. O. Jeschke, Phys. Rev. B **86**, 195119 (2012), URL http://link.aps.org/doi/10.1103/PhysRevB.86.195119.

[38] C. Lin, C. Mitra, and A. A. Demkov, Phys. Rev. B **86**, 161102 (2012), URL http://link.aps.org/doi/10.1103/PhysRevB.86.161102.

[39] Y. Aiura, I. Hase, H. Bando, T. Yasue, T. Saitoh, and D. S. Dessau, Surf. Sci. **515**, 61 (2002).

[40] N. W. Ashcroft and N. D. Mermin, *Solid State Physics* (Saunders College Publishing, 1976), see Ch. 10 for the tight-binding approximation.

[41] Because the t_{2g} levels of Ti next to OV do not change much in the LDA+U calculation [36], we neglect this effect.

[42] The contribution from $\langle 3d_{xy}|y|3d_{3x^2-r^2}\rangle$ is zero, because the integrand is an odd function in x.

[43] We use $\phi_{4p_x}(\mathbf{r}) = R_{n=4,l=1}(r)\left(\sqrt{\frac{3}{4\pi}}\frac{x}{r}\right)$ and $\phi_{3d_{xy}}(\mathbf{r}) = R_{n=3,l=2}(r)\left(\sqrt{\frac{15}{4\pi}}\frac{xy}{r^2}\right)$ with n, l the principle and angular quantum numbers respectively.

[44] For a point charge e, the electric field 3.8Å (about one lattice constant) away from the origin is about 1eV/1Å. As this certainly overestimates the stray field, we take half of this value.

[45] For uniform surface charge, the in-plane eletric field components are zero and no coupling is induced.

[46] The stray electric field decays like $1/r^2$ within a few Å, and faster when the electron and lattice screening start to take effect at longer distance. Note that the coupling $|g|$ is proportional to E; the Kondo temperature $T_K \sim e^{-J\rho_0}$ with $J \sim g^2$ some constant; the Curie temperature $T_c \sim J \sim g^2$. Both effects decay fast away from the top layer due to the decreasing $|g|$.

[47] P. W. Anderson, Phys. Rev. **124**, 41 (1961), URL http://link.aps.org/doi/10.1103/PhysRev.124.41.

[48] J. Lee and A. A. Demkov, Phys. Rev. B **78**, 193104 (2008), URL http://link.aps.org/doi/10.1103/PhysRevB.78.193104.

[49] G. Khalsa and A. H. MacDonald, Phys. Rev. B **86**, 125121 (2012), URL http://link.aps.org/doi/10.1103/PhysRevB.86.125121.

[50] S. Y. Park and A. J. Millis, Phys. Rev. B **87**, 205145 (2013), URL http://link.aps.org/doi/10.1103/PhysRevB.87.205145.

[51] Due to the low filling of the conduction band, all types of density-density interaction between the impurity and Ti $3d_{xy}$ orbitals can be safely neglected. The FM spin coupling between them (Hund's coupling) is neglected because the Ti orbitals next to OV are spatially extended (compared to those without OV) so that the Hund's coupling is weakened.

[52] From Fig. 1(b), in the spatial region between two Ti, the left Ti $3d_{xy}$ orbital has a plus/minus sign in the $+y/-y$ region, opposite to that of the right Ti. As the impurity orbital is symmetric between $+y/-y$, an opposite electric field is needed to give the same coupling g. For a uniform field, the couplings are opposite in sign.

[53] H. R. Krishna-murthy, J. W. Wilkins, and K. G. Wilson, Phys. Rev. B **21**, 1003 (1980), URL http://link.aps.org/doi/10.1103/PhysRevB.21.1003.

[54] A. Weichselbaum and J. von Delft, Phys. Rev. Lett. **99**, 076402 (2007), URL http://link.aps.org/doi/10.1103/

PhysRevLett.99.076402.

[55] T. A. Costi, A. C. Hewson, and V. Zlatić, J. Phys. C **6**, 2519 (1994).

[56] R. Bulla, T. A. Costi, and T. Pruschke, Rev. Mod. Phys. **80**, 395 (2008), URL http://link.aps.org/doi/10.1103/RevModPhys.80.395.

[57] NRG parameters defined in Ref.[53] are summarized as follows. The half bandwidth D is 0.2eV. The on-site correlation $U/D = 8$; the impurity-bath coupling is described by $\Gamma = \pi\rho_0(\sqrt{2}g)^2/D = 0.4$ or $V = \sqrt{2\Gamma/\pi} \sim 0.5$. The parameter with respect to the logarithmic discretization Λ is 2. We keep at least 2000 states at each NRG iteration.

[58] The Wilson ratio being two indicates that the charge degree of freedom is totally frozen, i.e the impurity occupation is always one. It corresponds to the large $U/|g|$ limit.

[59] J. R. Schrieffer and P. A. Wolff, Phys. Rev. **149**, 491 (1966), URL http://link.aps.org/doi/10.1103/PhysRev.149.491.

[60] A. C. Hewson, *The Kondo Problem to Heavy Fermion* (Cambridge University Press, 1993).

[61] M. A. Ruderman and C. Kittel, Phys. Rev. **96**, 99 (1954), URL http://link.aps.org/doi/10.1103/PhysRev.96.99.

[62] K. Yosida, Phys. Rev. **106**, 893 (1957), URL http://link.aps.org/doi/10.1103/PhysRev.106.893.

[63] B. Fischer and M. W. Klein, Phys. Rev. B **11**, 2025 (1975), URL http://link.aps.org/doi/10.1103/PhysRevB.11.2025.

[64] V. I. Litvinov and V. K. Dugaev, Phys. Rev. B **58**, 3584 (1998), URL http://link.aps.org/doi/10.1103/PhysRevB.58.3584.

[65] $J_{RKKY,xa}(\mathbf{R})$ is given by $\frac{J^2}{N^2}\sum_{k<k_f,k'>k_f}\frac{e^{i(\mathbf{k}-\mathbf{k}')\cdot\mathbf{R}}f(\mathbf{k},\mathbf{k}';x)f^*(\mathbf{k},\mathbf{k}';a)}{\varepsilon_{\mathbf{k}}-\varepsilon_{\mathbf{k}'}}$. Here N is the total number of lattice sites and $f(\mathbf{k},\mathbf{k}';a)$ is $2\cos(\mathbf{k}\cdot\hat{a}/2)\cos(\mathbf{k}'\cdot\hat{a}/2)e^{i\mathbf{k}\cdot\hat{a}/2}e^{-i\mathbf{k}'\cdot\hat{a}/2}$.

[66] C. Zener, Phys. Rev. **82**, 403 (1951), URL http://link.aps.org/doi/10.1103/PhysRev.82.403.

[67] J. Park, B.-G. Cho, K. D. Kim, J. Koo, H. Jang, K.-T. Ko, J.-H. Park, K.-B. Lee, J.-Y. Kim, D. R. Lee, et al., Phys. Rev. Lett. **110**, 017401 (2013), URL http://link.aps.org/doi/10.1103/PhysRevLett.110.017401.

[68] M. Salluzzo, S. Gariglio, D. Stornaiuolo, V. Sessi, S. Rusponi, C. Piamonteze, G. M. De Luca, M. Minola, D. Marré, A. Gadaleta, et al., Phys. Rev. Lett. **111**, 087204 (2013), URL http://link.aps.org/doi/10.1103/PhysRevLett.111.087204.

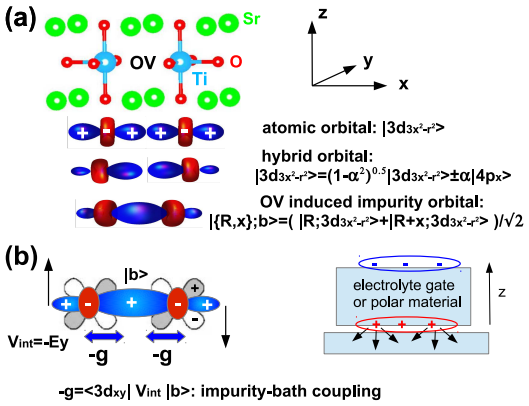

FIG. 1: (Color online) (a) Without vacancies, the local $|3d_{3x^2-r^2}\rangle$ orbital is symmetric with respect to the Ti site. A vacancy lowers the local symmetry to C_{4v}, and an hybrid state involving $4p$ component forms. The OV-induced bonding state is the lowest single particle level induced by an OV [Eq. (1)]. The blue/gray and red/white indicate the signs of wave functions. (b) The inhomogeneous surface charge from the ionic liquid gate or polar materials can cause a local strong electric field. The coupling between the impurity and conduction band becomes non-zero when an external electric field is present. The arrows indicate the directions of the electric fields at two Ti sites.

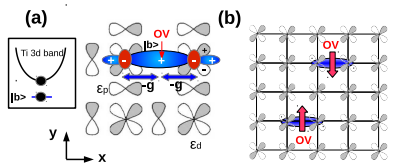

FIG. 2: (Color online) (a) The bath orbitals are composed of Ti $3d_{xy}$, O $2p_x$, O $2p_y$ orbitals (of energies ε_d, ε_p). The OV-induced bonding state $|b\rangle$ can couple to two Ti $3d_{xy}$ orbitals across the OV. The coupling g can be non-zero near the interface. The inset illustrates relative energies of the conduction band and the impurity levels. (b) The tight-binding band composed of Ti $3d_{xy}$ orbitals only. The OV-induced orbital, represented by a local spin, is localized between two adjacent lattice sites (the bond).

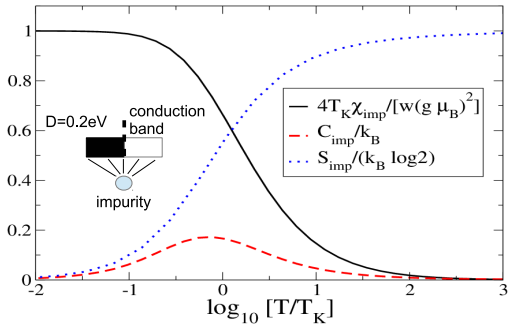

FIG. 3: (Color online) The scaled magnetic susceptibility $4T_K\chi_{imp}/[w(g\mu_B)^2]$ (w the Wilson number, ~ 0.413), specific heat C_{imp}/k_B (red dashed), and the entropy $S_{imp}/(k_B \log 2)$ (blue dotted) for a single OV impurity as a function of temperature. All quantities are dimensionless and computed using the numerical renormalization group method, as illustrated in the inset.

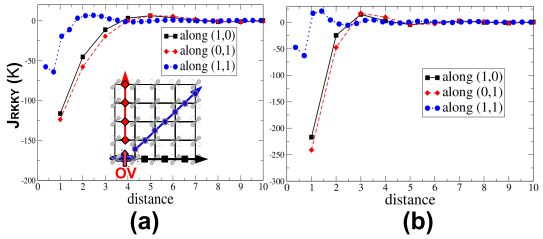

FIG. 4: (Color online) The RKKY magnetic coupling in Kelvin between two local impurities for two electron fillings (per spin per site): (a) $n_{2D} = 0.015$ and (b) $n_{2D} = 0.05$. The distance is in the unit of lattice constant. The negative values favor FM coupling. The inset of (a) indicates the three scanning directions – (1,0), (0,1), (1,1) are represented by square, diamond, and circle ligands respectively.